THE ASTROPHYSICAL JOURNAL, 392:201–208, 1992 June 10

Hα OBSERVATIONS OF EARLY-TYPE STARS

S. SCUDERI
Istituto di Astronomia, Università di Catania, Viale Andrea Doria 6, I-95125 Catania, Italy
G. BONANNO, R. DI BENEDETTO, AND D. SPADARO
Osservatorio Astrofisico di Catania, Viale Andrea Doria 6, I-95125 Catania, Italy
AND
N. PANAGIA[1,2]
Space Telescope Science Institute, and University of Catania
Received 1991 July 18; accepted 1991 December 16

ABSTRACT

We present the results of a first session of a program run at the Catania Astrophysical Observatory to study and monitor the Hα emission from early-type stars and determine the properties of their mass loss. Twelve early-type supergiants in the Cygnus region were observed repeatedly in 1988 July. From these observations we find evidence for short-term variability of the mass-loss rate, Also, a comparison with literature data reveals strong long-term variations for some of the stars. We have also developed simplified models to describe the Hα profile resulting from the combination of photospheric absorption with emission and scattering in the wind. By fitting the observed profiles with our models we determine the mass-loss rates and the velocity fields for all stars with accuracies generally better than 25%.

Subject headings: stars: early-type — stars: emission-line — line: profiles — stars: mass loss — supergiants

1. INTRODUCTION

The winds from early-type stars are known to be mostly ionized and to absorb a sizable fraction of the Lyman continuum ionizing radiation (e.g., Felli & Panagia 1981a). Therefore, it is clear that stellar winds are prime sources of recombination line radiation: in particular, strong Hα emission may be expected in the optical spectrum. Actually, pioneering works of the Hα emission from stellar winds (Castor & Klein 1978; Ebbett 1982; Leitherer 1988) have already shown its great potential for the study of the mass loss from early-type stars.

Within this frame, at Catania Observatory we have started a program of systematic Hα observations of early-type stars aiming at three main goals: (i) to determine the properties of their steady winds; in particular, the mass-loss rate $\dot{M}$ and the velocity field $v(r)$; (ii) to monitor and study the time variability of mass loss; (iii) to study the distribution of wind material in/around close binary systems.

The sample consists of all O and B supergiants accessible in the northern sky, for which IR and/or radio data exist and that are brighter than 11.5 mag: this amounts to a total of 56 stars.

We are planning to have observing runs of 1 week–10 days spaced by about 3 months from each other. With this strategy, weather permitting, all stars can be observed at least in two runs every year and several nights per run. Therefore, we will be able to study possible variability on time scales from few hours through few days to several months and possibly, years. So far, we have had six successful runs, in 1988 July, in 1989 June and September/October and 1990 January, April. and August. Next run will be in 1991 July/August.

Here we report on the result of our observations made in 1988 July that include 12 early-type stars in the Cygnus region. We find evidence for appreciable variability in several cases. By using new model calculations and fitting the observed profiles we determine the mass-loss rates and the velocity fields in the winds of the program stars. Also, we find evidence that the O3 If star Cyg OB2 No.7 may be a high-velocity runaway star which could have been member of a binary system in which the primary had a mass in excess of 100 $M_\odot$ and exploded less than 10^5 yr ago.

2. INSTRUMENTAL APPARATUS

The basic observing apparatus consists of an echelle spectrograph and a CCD detector attached to the 91 cm telescope of the Catania Astrophysical Observatory at Serra La Nave. The echelle spectrograph offers two possible configurations:

1. "Low-dispersion mode" that uses only an echelette grating (1200 gr mm^{-1}), giving a reciprocal dispersion of 40 Å mm^{-1};
2. "High-dispersion mode" that uses an echelle grating (79 gr mm^{-1}), giving a reciprocal dispersion ranging from 5 to 10 Å mm^{-1}.

The spectrograph is optimized to be placed on the Cassegrain focal plane (F/15) of the 91 cm telescope. The camera has a 20 cm focal length and an F/1.46 aperture. The corrected field on the focal plane of the spectrograph is 28.5 × 19 mm^2. The accessible spectral range is 3450–6800 Å. The CCD detector and data handling system, developed at Catania Astrophysical Observatory, consists of a CCD matrix of 385 × 576 pixels (pixel size: 22 × 22 μm^2) front-illuminated inside a dewar, an electronic controller-interface, and a PDP 11/24 computer equipped with a magnetic tape unit to store the CCD images (see Bonanno & Di Benedetto 1990). The main features of the system can be summarized as follows: the deviation from linearity of the detector is below 0.5% over the whole dynamic

[1] Affiliated to the Astrophysics Division of the Space Science Department of ESA.
[2] Postal address: Space Telescope Science Institute, 3700 San Martin Drive, Baltimore, MD 21218.

range; the analog-to-digital (A/D) converter has a 12 bit of resolution; the conversion factor (electrons per A/D units) is 2.42; the adopted pixel scanning time is 120 μs; the read-out noise is 12 electrons rms; the response quantum efficiency in the spectral region of Hα is 45%; the CCD has a good charge transfer efficiency and a good uniformity over the whole sensitive surface; the CCD camera link with the computer interface is realized via an optical fiber: this avoids the problems due to the electromagnetic noise produced by the various driving devices.

The system was used in the "low-dispersion mode." In this case the spectrum is dispersed along the major dimension of the CCD and the corresponding characteristics are spectral dispersion equal to 0.89 Å pixel^{-1} and covered spectral range of 450 Å.

Because of the low quantum efficiency of the CCD in the blue region and the 6800 Å operating wavelength limit of the spectrograph, the system has the highest efficiency in the Hα region (6270–6720 Å).

The actual spectral resolution of the whole system (telescope + spectrograph + CCD) is limited by the pixel size, because the width of the entrance slit corresponds on the focal plane to approximately the pixel width. Therefore, we will consider the spectral resolution to be equal to 0.89 Å which at the Hα wavelength corresponds to 40 km s^{-1}.

3. OBSERVATIONS AND DATA REDUCTION

The log of the observations is presented in Table 1. The stars were observed with exposure times ranging from 2 to 300 s, so as to give a signal-to-noise ratio of about 50. The stellar spectra, calibrated in wavelength, were obtained from the CCD camera images through the following steps:

a. Subtraction of the electronic bias, which was estimated by using a region of the CCD matrix insensitive to radiation;

b. Division by the spectrum of the flat-field lamp, in order to remove the effects of differences in sensitivity between adjacent pixels;

c. Subtraction of the sky background which was estimated by using a region not exposed to the stellar radiation;

d. Addition of the counts in 6 or 8 (depending on the "seeing figure") adjacent pixels along columns perpendicular to the wavelength dispersion, to obtain the stellar flux per unit wavelength interval, in arbitrary units, versus pixel number along dispersion (in fact, owing to the "seeing," the radiation from a star is distributed along the spectrometer entrance slit so as to cover more than one pixel);

TABLE 1

LOG OF THE OBSERVATIONS

Star	Observation Date (1988)	Recorded Spectra
Cyg OB2 No. 7	Jul 10	1
HD 190429 A	Jul 7	2
Cyg OB2 No. 8A	Jul 11	2
HD 193514	Jul 7	2
HD 188001—9 Sge	Jul 5, 10	2, 2
BD −11 4586	Jul 7	2
HD 167330	Jul 5, 11	2, 2
HD 188209	Jul 8	2
HD 193237—P Cyg	Jul 5, 10	2, 1
HD 197345—α Cyg	Jul 7	2
HD 166734	Jul 5, 8	2, 2
Cyg OB2 No. 5	Jul 5, 10, 12	2, 2, 2

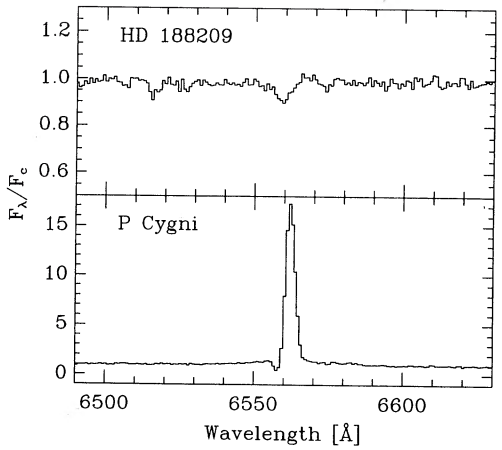

FIG. 1.—Hα region of P Cygni and HD 188209. Spectra are normalized to the continuum level. Note the presence of interstellar absorption lines of H_2O 6513 Å and diffuse interstellar band 6613 Å, as well as He II 6527 Å and He I 6678 Å photospheric/wind lines.

e. Wavelength calibration, through the observation of the spectrum of a Cs calibration lamp and the identification of the Cs lines in the spectral region of Hα by means of Striganov & Sventitskii (1968) tables.

To analyze the spectra we have first normalized the stellar continuum to a unity level, by using an algorithm developed by Keith Horne at the Space Telescope Science Institute. Some examples of normalized spectra are displayed in Figure 1. It provides an illustration of the possible cases, i.e., from extremely strong Hα line with a very prominent emission and a nominal absorption, as for P Cyg (B1 Ia$^+$), to HD 188209 (O9.5 I) that exhibits a broad and shallow Hα absorption line indicative of photospheric absorption partially filled-in by wind emission.

From these spectra we have measured the equivalent widths of the Hα line. The accuracy of these determinations is limited by uncertainties in the measured flux and, more importantly, by uncertainties in the definition of the level of the continuum (typically of the order of 1%–2% of the continuum flux). The estimated errors in the equivalent widths are all of the order of few tenths of an angstrom.

For each star, except Cyg OB2 No. 7, we have at least two spectra taken at different epochs. Since the differences among the values are within the errors, the equivalent widths given in Table 2 are generally straight averages of the available values.

Only for HD 167330 are there significant variations of the equivalent width between the nights of July 5 and 11. Also, the profile is seen to vary somewhat (see Fig. 2). Therefore, for this star we report two values of W_{eq}, 0.92 and 0.59 Å, respectively, for the nights of July 5 and 11.

In addition, there are objects for which, although the differences in the Hα equivalent widths are comparable to the errors, we find evidence for short-term (few days) intrinsic variability of the Hα emission. This is the case of HD 188001 (9 Sge), whose normalized spectra are shown in Figure 3. The spectrum, taken on July 10, presents an absorption feature in the blue wing of the Hα profile, which is absent in the spectrum obtained on July 5.

The cases of Cyg OB2 No. 5 (BD +40°4220) an HD 166734 are different: these objects are binary stars, so that the differences between the Hα profiles obtained at different epochs (see Figs. 4 and 5) can be related to the orbital motion of the two

TABLE 2

Hα EQUIVALENT WIDTHS

Star	Spectral Type	W_{eq} (Å)	$\sigma_{W_{eq}}$ (Å)	W_{eq} (Å)	W_{phot} (Å)	$-W_{wind}$ (Å)
Cyg OB2 No. 7	O3 If	0.72	0.36	−0.8[a]	2.80	2.43
HD 190429 A	O4 If	−2.20	0.52	−7.9[b]	2.63	4.87
Cyg OB2 No. 8A	O6 If	0.68	0.30	−0.5[a], 0.31[c]	2.45	1.83
HD 193514	O7 If	0.51	0.12	0.3[d], 0.62[e]	2.48	2.14
HD 188001—9 Sge	O8 If	−2.42	0.38	−2.45[e], −3.52[f]	2.35	4.80
BD −11 4586	O8 I	0.33	0.14	...	2.42	2.13
HD 167330	O9 I	0.59	0.13	...	2.23	1.76
		0.92				1.51
HD 188209	O9.5 I	0.57	0.14	−0.27[f], −2.1[e]	2.17	1.73
HD 193237—P Cyg	B1 Ia$^+$	−65.2	0.51	−54.2[g,h]	1.22	66.5
HD 197345—α Cyg	A2 Ia	1.29	0.21	1.61[i]	2.77	1.61

[a] Abbott, Bieging & Churchwell 1981.
[b] Conti & Frost 1977.
[c] Leitherer et al. 1982.
[d] Peppel 1984.
[e] Conti 1974.
[f] Ebbets 1982.
[g] Bernat & Lambert 1978.
[h] Includes only core emission.
[i] Rosendhal 1973.

components. The discussion of these cases is deferred to a future paper after more observations are collected.

Table 2 lists the Hα equivalent widths and their uncertainties for the program stars, excluding Cyg OB2 No. 5 and HD 166734. The equivalent widths found in the literature for the same set of stars are also reported. We see that for most stars our W_{eq} values deviate from at least some of the other published values by more than the observational errors. In some cases our measurements agree with one of the values taken from the literature but not with another. We interpret these discrepancies as mostly due to genuine variability rather than inordinately large errors in the old measurements. Evidence for short- and long-term variability in the Hα intensity and profile of early-type stars had been noticed already by Ebbets (1982). Such a variability in early-type stars makes any statistical study of the stellar wind properties rather difficult unless an appropriate time coverage exists for *each* star of the sample under study. This fact justifies a posteriori our choice of monitoring the Hα line for a large sample of stars over a period of time of several years.

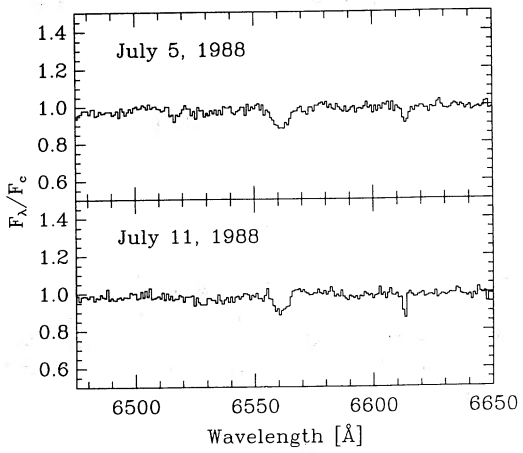

FIG. 2.—Normalized spectra of HD 167330, taken on July 5 and July 11.

4. STELLAR WIND PARAMETERS FROM Hα OBSERVATIONS

To use the Hα line for the diagnostic of stellar winds we have to solve the radiative transfer problem for the Hα line in the expanding envelope. In order to make this problem easily treatable, we have adopted the wind model developed by Panagia & Felli (1975), Felli & Panagia (1981a), and Panagia (1988). The basic assumptions are as follows:

1. The wind is spherically symmetric with a steady mass-loss rate $\dot{M}$.
2. The wind is fully ionized.
3. The wind velocity, v, increases with the radius, r, like a power law of exponent γ, until it reaches its terminal value v_∞ at a radius R_1, and constant afterward:

$$v = v_0\left(\frac{r}{R}\right)^\gamma \qquad r \le R_1 = R\left(\frac{v_\infty}{v_0}\right)^{1/\gamma} \tag{1}$$

$$v = v_\infty \qquad r \ge R_1\,, \tag{2}$$

where v_0 and R are the initial velocity and the radius of the star, respectively.

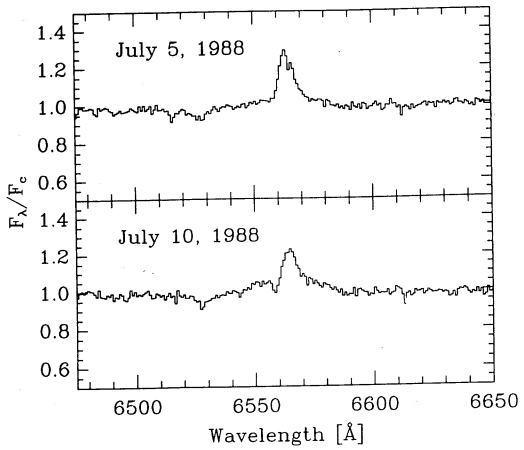

FIG. 3.—Normalized spectra of HD 188001 (9 Sge), taken on July 5 and July 10.

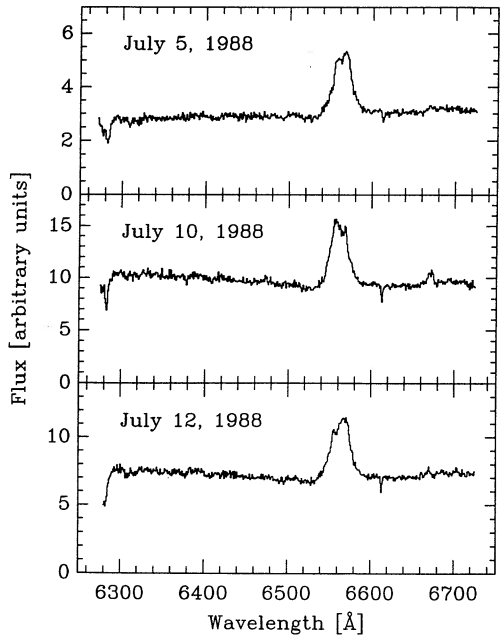

FIG. 4.—Spectrum of Cyg OB2 No. 5 on 1988 July 5, July 10, and July 12

4. The wind is isothermal at the same temperature as the stellar photosphere (assumed equal to $0.85 \times T_{\rm eff}$, with $T_{\rm eff}$ effective temperature of the star).

5. Quasi–LTE conditions hold, i.e., the Kirchhoff law applies.

6. The Hα line radiation transfer is treated adopting the Sobolev approximation (Sobolev 1958) because the wind velocity is considerably higher than the gas thermal velocity.

7. The Hα line opacity is much larger than that of the continuum so that their radiative transfer problems in the wind are completely decoupled.

With these assumptions the intrinsic emission produced by the wind in the Hα line at a frequency ν is given by (e.g., Panagia 1988):

$$L_\nu = 4\pi R^2 \pi B(\nu_0) \times 2 \int_1^\infty (1 - e^{-\tau(\nu,\xi)})\xi \, d\xi \quad \text{ergs s}^{-1}\ \text{Hz}^{-1}\,, \tag{3}$$

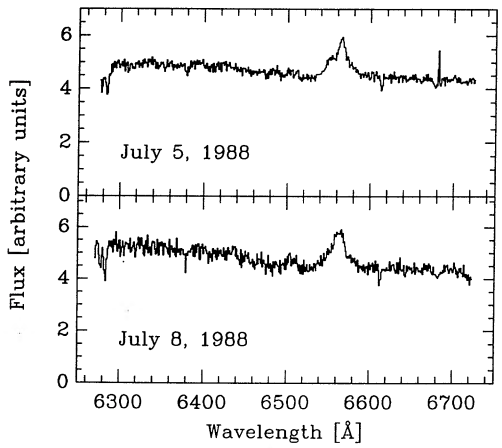

FIG. 5.—Spectrum of the binary system HD 166734 on 1988 July 5 and July 8

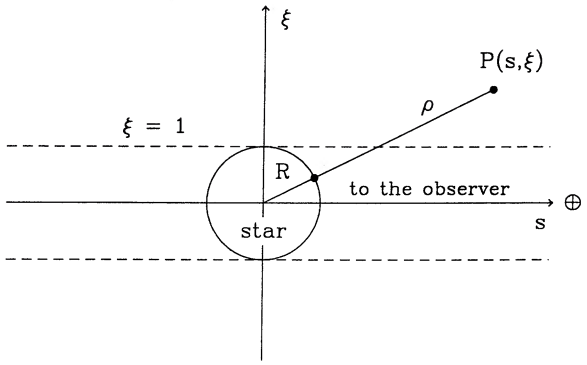

FIG. 6.—Geometry of the star–wind system.

where $B(\nu_0)$ is the Planck function at $T = T_{\rm wind}$ and at the rest frequency of the Hα line, ν_0. The wind optical depth in the Hα line, as a function of the frequency and the wind parameters, can be expressed as (Castor 1970)

$$\tau(\nu, \xi) = \tau_0 \frac{\rho^{-3(\gamma+1)}}{1 + s^2(\gamma - 1)/\rho^2}\,, \tag{4}$$

where γ is exponent of the velocity law, and ρ, s, ξ are the coordinates in units of the stellar radius (see Fig. 6, which illustrates the adopted geometry of the star–wind system) of a generic volume element in the expanding envelope. The quantity τ_0 is the optical depth at the center of the line and for $\xi = 1$, defined as (Castor 1970):

$$\tau_0 = \frac{\pi e^2}{mc} g_2 f_{23} \frac{(n_2/g_2) - (n_3/g_3)}{v_0(v_0/c)} R\,, \tag{5}$$

where n_2, n_3, and g_2, g_3 are the populations and the statistical weights of the second and third level of neutral hydrogen, respectively. Note that in the case of hydrogen lines, and in particular the Hα line, the population of the excited levels is proportional to the square of the electron density, so that τ_0 is proportional to the product $\dot{M}^2/(v_0^3 R^3)$ (Panagia 1988).

As we can see from equations (3)–(5), the profile of the Hα line emitted by the wind depends mostly on γ and, through τ_0, on $\dot{M}$ and v_0.

The integrated line luminosity emitted by the wind is then given by

$$L_{\rm tot}({\rm H}\alpha) = 8\pi^2 R^2 B(\nu_0) \frac{v_0 v_0}{c} A(\tau_0, \gamma) \quad \text{ergs s}^{-1} \tag{6}$$

where

$$A(\tau_0, \gamma) = \int_1^{v_\infty/v_0} f[\tau(v)] d\left(\frac{v}{v_0}\right), \tag{7}$$

and

$$f(\tau) = \int_1^\infty (1 - e^{-\tau})\xi \, d\xi\,. \tag{8}$$

Since the equivalent width of a line is the ratio of its total luminosity to the average continuum flux at the same wavelength, the equivalent width of the Hα emission due to the wind, $W_{\rm wind}$, is simply related to the quantity $A(\tau_0, \gamma)$ defined by equation (7):

$$\frac{W_{\rm wind}}{(\lambda_0 v_0/c)} = 2A(\tau_0, \gamma)\,. \tag{9}$$

Solving this equation one can determine the value of τ_0 from the line equivalent width, once v_0 and γ are given. Before doing this, however, one has to allow for the contribution of a P Cyg-like line and for the photospheric absorption line.

The P Cyg-like line profile due to line photon scattering in the wind is calculated assuming the optical depth *not* to depend on the angle between a radius and the line of sight or, equivalently, taking the denominator in equation (4) to be identically unity for any value of γ. This means that the energy absorbed by the layers at radius ρ is simply a fraction $\{1 - \exp[-\tau_0 \rho^{-3(\gamma+1)}]\}$ of the stellar radiation at that frequency. Moreover, because of projection effects, the effects of the absorption produced in that shell will be distributed evenly over the velocity interval $(v_{\min}, v)$, where $v_{\min}$ is the shell velocity projected along the line of sight tangential to the star, i.e., at $\xi = 1$. Such a velocity can be evaluated as

$$v_{\min} = v \cos\theta = v \frac{s(\rho(v))}{\rho(v)} \tag{10}$$

which defining $y = v/v_0$, can be written as

$$y_{\min} = y^{(\gamma-1)/\gamma}(y^{2/\gamma} - 1)^{1/2} . \tag{11}$$

Therefore, absorption will affect only the blue profile and, at each *observed* velocity (i.e., projected velocity), absorption will be produced by layers moving at *radial* velocities between $v_{\text{radial}} = v_{\text{projected}}$ and a higher value $v_1 = v_{\text{projected}}/\cos\theta\,(\xi = 1)$. Denoting with x the observed velocity in units of the initial velocity (i.e., $x = v_{\text{projected}}/v_0$), such a velocity y_1 can be evaluated by solving the equation

$$y_1^2(1 - y_1^{-2/\gamma}) = x^2 . \tag{12}$$

The photons absorbed by a shell moving radially at velocity v will be reemitted isotropically and, therefore, with equal probability in the interval of projected velocities $(-v, v)$. Therefore, expressing the intensity in units of the stellar continuum, the blue profile of the line will be given by

$$I_{\text{blue}}(x) = 1 - \int_{\max(x,1)}^{y_1} \frac{1 - e^{-\tau(y)}}{y - y_{\min}}\, dy + \int_{\max(x,1)}^{y_\infty} \frac{1 - e^{-\tau(y)}}{2y}\, dy \tag{13}$$

where τ is the optical depth computed setting the denominator in equation (4) equal to unity, i.e.,

$$\tau = \tau_0 \rho^{-3(\gamma+1)} . \tag{14}$$

The first term in equation (13) represents the net effect of absorption in the wind and the second term accounts for the subsequent reemission.

Analogously, for the red side of the line profile there is only emission and, because of partial occultation by the star itself, the integration will extend from y_1 up to y_∞. Thus, we obtain

$$I_{\text{red}}(x) = \int_{y_1}^{y_\infty} \frac{1 - e^{-\tau(y)}}{2y}\, dy . \tag{15}$$

The P Cyg-like profile obtained in this manner is combined with the photospheric absorption profile adopting the approximation proposed by Castor & Lamers (1979). The photospheric profile is deduced from the grid of model atmospheres computed by Auer & Mihalas (1972), Mihalas (1972), and Kurucz (1979), interpolating among the available profiles for the corresponding surface gravity and effective temperature of the star. Finally, direct summation of the emission profile, obtained by numerically integrating equation (3), to the P Cyg one (equations [13] and [15]) gives the final profile to compare with observations.

The free parameters for a model fit to the observations are τ_0, v_0, and γ. First guess values are obtained by fitting the observed equivalent width, W_{eq}, the half-power width of the red profile and the line peak intensity. Then, the final values of the parameters are obtained with a minimum χ^2 fit of the whole profile.

The mass-loss rate can be deduced from the formula

$$\dot{M} = 0.203 \mu_e \left(\frac{\tau_0}{b_2}\right)^{1/2} \left[\frac{T_e}{10^4\ \text{K}}\right]^{3/4} \left[\frac{R}{10\ R_\odot}\right]^{3/2} \left[\frac{v_0}{100\ \text{km s}^{-1}}\right]^{3/2} \times (e^{E_2/kT} - e^{E_3/kT})^{-1/2}\ \ 10^{-6}\ M_\odot\ \text{yr}^{-1} , \tag{16}$$

where μ_e is the mean atomic weight per electron, equal to 1.3 for a fully ionized gas composed of 90% hydrogen and 10% helium, E_2 and E_3 are the ionization energies from the second and the third level of hydrogen, respectively, and b_2 is the ratio of the population of the second level to that in LTE. Following Klein & Castor (1978) we adopt $b_2 = 1.3$ in our calculations.

The uncertainty on τ_0 has been estimated attributing to W_{wind} the uncertainty on W_{eq} and using two analytical formulae given by Panagia (1988) to relate τ_0 to W_{wind} in the optically thin and optically thick cases

$$W_{\text{wind}}(\text{thin}) = 2\left[\frac{1 + J(\gamma)}{1 + 2\gamma}\right] \tau_0 \frac{v_0}{c} \lambda_0 , \tag{17}$$

$$W_{\text{wind}}(\text{thick}) = \frac{4}{2 + \gamma} \left\{\Gamma\left[1 - \frac{2}{3(\gamma + 1)}\right]\right\}^{1+\gamma/2} \times \tau_0^{(2+\gamma)/3(1+\gamma)} \frac{v_0}{c} \lambda_0 , \tag{18}$$

where Γ is the Euler function and $J(\gamma)$ is defined as

$$J(\gamma) = \frac{\sqrt{\pi}}{2} \frac{\Gamma(\gamma + 3/2)}{\Gamma(\gamma + 2)} .$$

Thus, equation (16) can be expressed in the optically thin limit as

$$\dot{M}(\text{thin}) = 0.11 \left[\frac{1 + 2\gamma}{1 + J(\gamma)}\right]^{1/2} \left(\frac{b_2}{1.3}\right)^{-1/2} \left[\frac{W_{\text{wind}}}{\text{Å}}\right]^{1/2} \times \left[\frac{v_0}{100\ \text{km s}^{-1}}\right] \left[\frac{R}{10\ R_\odot}\right]^{3/2} \left[\frac{T_e}{10^4\ \text{K}}\right]^{3/4} \times (e^{3.94/T_4} - e^{1.75/T_4})^{-1/2}\ \ 10^{-6}\ M_\odot\ \text{yr}^{-1} \tag{19}$$

and in the optically thick limit as

$$\dot{M}(\text{thick}) = 0.231 \left\{\Gamma\left[1 - \frac{2}{3(\gamma + 1)}\right]\right\}^{-3/4(1+\gamma)} \left[\frac{b_2}{1.3}\right]^{-1/2} \times \left\{0.457 \frac{(\gamma + 2)}{4} \left[\frac{v_0}{100\ \text{km s}^{-1}}\right]^{-1} \times \left[\frac{W_{\text{wind}}}{\text{Å}}\right]\right\}^{3(1+\gamma)/2(2+\gamma)} \left[\frac{v_0}{100\ \text{km s}^{-1}}\right]^{3/2} \left[\frac{R}{10\ R_\odot}\right]^{3/2} \times \left[\frac{T_e}{10^4\ \text{K}}\right]^{3/4} (e^{3.94/T_4} - e^{1.75/T_4})^{-1/2}\ \ 10^{-6}\ M_\odot\ \text{yr}^{-1} . \tag{20}$$

These formulae provide the explicit functional dependence of $\dot{M}$ on both the *measured* and the *adopted* quantities and, therefore, are convenient to estimate its overall uncertainty. In equation (19) $\dot{M}$ depends on the square root of $W_{\rm wind}$, the first power of velocity, the 1.5 power of the stellar radius and, to a first-order approximation, on the second power of the temperature. In the optically thick case (eq. [20]) the functional dependence of $\dot{M}$ on stellar radius and temperature remains unchanged i.e., 1.5 and 2 powers, respectively, while now $\dot{M}$ depends on the square or third root of the velocity and essentially linearly on the equivalent width.

Moreover, equations (19) and (20) are handy for a quick evaluation of the mass loss rate from Hα measurements, which is especially accurate when the line is *seen* in emission. In fact, $W_{\rm wind}$ is essentially the observed value, $W_{\rm eq}$, added of the expected $W_{\rm phot}$ due to photospheric absorption (see Table 2). The P Cyg line contribution can usually be ignored because it is significantly different from zero only for a high wind opacity, i.e., just when the emission is also high and, therefore, its contribution becomes negligible. We have checked that this approximate procedure can reproduce our exact results to within 15% for $W_{\rm wind}$ and within 30% for $\dot{M}$.

5. RESULTS AND DISCUSSION

The best fits to the line profiles of the program stars are shown in Figure 7. It is clear that the models reproduce the observations quite well, in most cases well within the measurement uncertainties. The only cases with incomplete agreement between observation and theory are those of HD 190429 and P Cyg. For the former our models predict an emission bump which is not seen in the observed spectrum; for the latter the observed profile shows a blue absorption which is not reproduced by the model. In both cases, however, the bulk of the line is still excellently fitted suggesting that one should simply make some small ad hoc adjustments to the models. Both stars have high mass loss rates and both are known to be variable: it is quite possible that releasing the assumption of a *steady* wind, a better agreement with observations would be found. This however, goes beyond the scope of our paper and is not attempted here.

While matching the models to the observations small adjustments to the wavelength, thus to the velocity scale, were required. In all cases, except Cyg OB2 No. 7, they were comparable to, or smaller than the velocity sampling step of 40 km s^{-1}, i.e., $\delta v = +2 \pm 42$ km s^{-1}. Moreover, the correctness of the wavelength scale was confirmed by the observed wavelengths of some interstellar features, such as H_2O 6513 Å and the unidentified diffuse interstellar band at 6613.6 Å (Herbig 1975) which in the Hα rest frame fall at -2276 and $+2322$ km s^{-1}, respectively. The latter is particularly suited for this purpose because it is rather narrow and can provide an external calibration of the wavelength scale to within few km s^{-1}.

In the case of Cyg OB2 No. 7, however, the required shift of the velocity scale is -230 km s^{-1}, which is much larger than any expected uncertainty. The position of the 6613 Å diffuse interstellar band seems to confirm the reality of this strongly negative velocity although we cannot completely rule out the possibility that the relatively high scatter in the observed profile be responsible for the apparent shift. Pending confirmation with more accurate observations, we speculate that Cyg

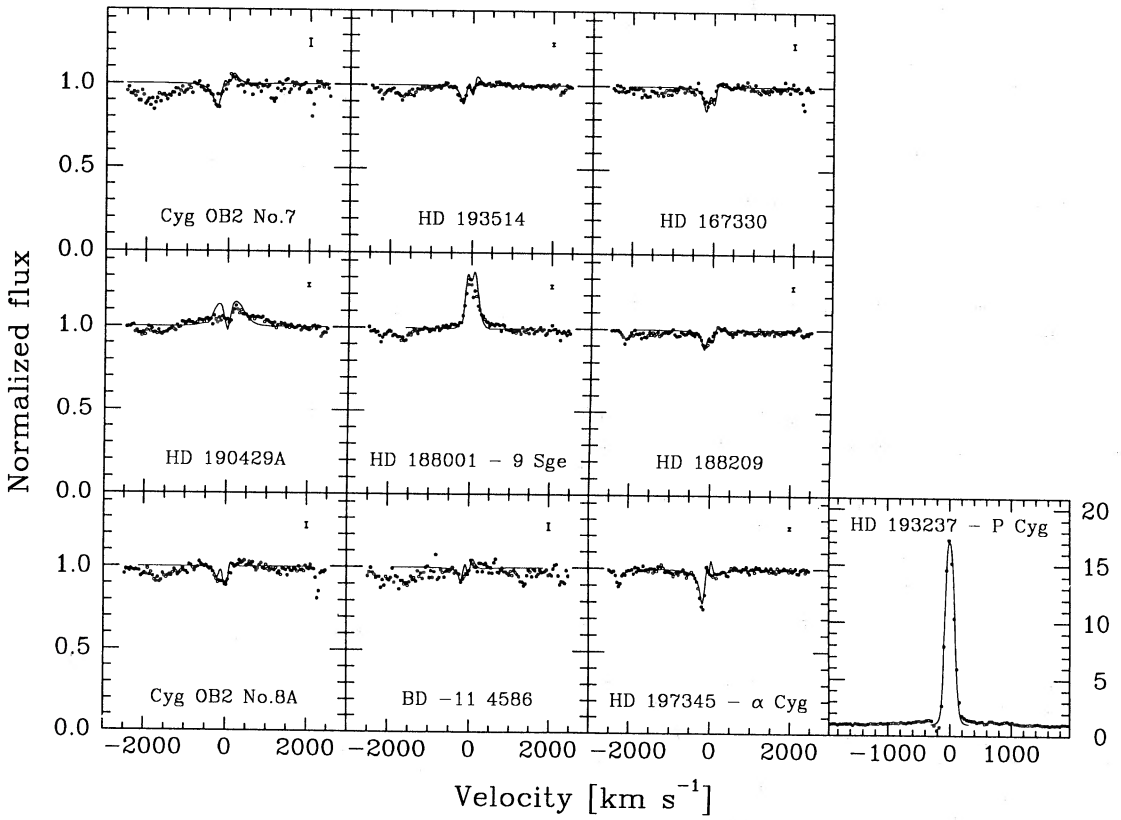

FIG. 7.—Observed profiles (*open dots*) are compared with model calculations (*solid lines*). Adopted parameters are those reported in Table 3.

TABLE 3

FINAL RESULTS

Star	Spectral Type	$T_{\rm eff}$ (K)	R ($R_\odot$)	$v_{\rm sound}$	v_0 (km s^{-1})	v_∞	γ	τ_0	$\dot{M}$	$\Delta\dot{M}$	$\dot{M}$ (radio) (10^{-6} $M_\odot$ yr^{-1})	$\dot{M}$(Hα)
Cyg OB2 No. 7	O3 If	47300	17	29	290	3650[a]	2.0	1.09	7.2	2.1	≤19.0[d]	13.1[h], 7.6[a]
HD 190429 A	O4 If	44100	19	28	440	2850[a]	0.5	0.39	8.6	1.5	<21.0[e]	12.6[a]
Cyg OB2 No. 8A	O6 If	39000	30	27	212	3200[a]	1.0	0.53	5.4	1.4	3.5[d]	3.9[h], 9.1[a]
HD 193514	O7 If	35700	20	25	230	2950[a]	1.5	0.87	3.6	0.7		3.2[i], 2.8[a]
HD 188001—9 Sge	O8 If	34200	24	25	200	2300[a]	0.5	0.89	3.7	0.6		4.1[a]
BD −11 4586	O8 I	34200	22	25	186	2700[b]	1.0	0.72	2.6	0.7	<14.4[f]	
HD 167330	O9 I	32600	23	24	197	2350[b]	2.0	0.98	3.2	0.6		
					182		1.5	0.90	2.8	0.5		
HD 188209	O9.5 I	32000	26	24	195	2100[a]	1.5	0.83	3.4	0.6	<21.0[g]	1.9[a]
HD 193237—P Cyg	B1 Ia$^+$	20800	78	19	57	310[a]	0.5	212	19.3	2.3	13.0[d]	
HD 197345—α Cyg	A2 Ia	9750	196	13	170	250[c]	2.0	1.25	3.7	0.8		

[a] Leitherer 1988.
[b] Estimated by means of an average $v_\infty - T_{\rm eff}$ relationship given by Panagia & Macchetto 1982.
[c] Lamers et al. 1978.
[d] Abbott, Bieging and Churchwell 1981.
[e] Abbott et al. 1980.
[f] Felli and Panagia 1981b.
[g] Vallée and Moffatt 1985.
[h] Leitherer et al. 1982.
[i] Peppel 1984.

OB2 No. 7 be a runaway star, possibly the companion of a more massive star that exploded as a supernova some 10^5 yr ago. This corresponds to the time required to cross the Cyg OB2 association assuming the transverse velocity to be equal to the radial velocity. The interest of such a result is that Cyg OB2 No. 7 is an O3 type star with a mass of about 90 $M_\odot$ (Leitherer 1988) and, therefore, its companion had to be even more massive in order to be the first one to explode as a supernova. This would offer a unique opportunity to determine the characteristics of the explosion of a documentedly very massive star. Detailed studies of Cyg OB2 No. 7 and its environment are in progress (Panagia and Scuderi, 1991).

The values of τ_0, v_0, γ, $\dot{M}$ and the uncertainty on $\dot{M}$, as well as the adopted values of the effective temperature and the stellar radius, are presented in Table 3. We adopt the effective temperatures and the stellar radii as given by Leitherer (1988), except in the case of α Cyg, for which the effective temperature is taken from Barlow & Cohen (1977). The uncertainty on the mass loss rate has been computed assuming a 5% uncertainty on both $T_{\rm eff}$ and R and 10% on v_0. We would like to stress that the value of the mass-loss rate depends not only on quantities which are either directly observed or derived from Hα observations, such as τ_0 or γ but also, and quite strongly, on assumed quantities, such as the stellar radius. We also note that our determination of the mass loss is only *apparently* independent of the distance. Actually, the distance to each star enters implicitly through the adopted value of the stellar radius, which, in turn, is the value appropriate for the spectral type of each star. Therefore, one should regard these mass loss determinations as distance dependent: the distance is essentially a spectroscopic distance and the functional dependence is the same as for the stellar radius in the above formulae (18), (19), and (20), i.e., $\dot{M} \propto d^{1.5}$. This is a result of general validity that applies to all cases in which the mass loss rate is derived from the estimate of an optical depth whose opacity is proportional to the density squared.

In all cases high values of the initial velocity are obtained, which are 3–10 times higher than the sound speeds in the stellar photospheres, $v_{\rm sound}$, and about 10 times lower than the terminal velocities v_∞ (see Table 3). This result suggests that the outflowing material undergoes a very fast initial acceleration between $v_{\rm sound}$ and the observed values of hundreds of km s^{-1} for v_0 and has a more gradual increase afterward. An alternative explanation for having high speeds near the stellar photosphere would be to invoke the presence of strong turbulence, as proposed by Groenewegen & Lamers (1989). In this case, however, one should face the problem of having at/near the stellar surface either random motions or velocity disturbances an order of magnitude higher than the sound speed, which is hard to justify in physical terms.

The values of the velocity law exponent γ fall in the interval 0.5 to 2 for all stars, with no obvious dependence of γ on spectral type. It is worth noting that the γ value derived here for P Cyg from Hα data agrees very well with the determination made by Felli et al. (1985) from an analysis of near-infrared lines and continuum.

Relative to the formalism which expresses the velocity in the form $v/v_\infty = 0.01 + 0.99(1 - R/r)^\beta$, our values of γ correspond to values of β of the order of unity: in particular $\beta = 1$ with a turbulent velocity about 1/10 the terminal velocity corresponds approximately to $\gamma \sim 2$; lower values of β correspond to higher γ, and vice versa. Therefore, our Hα data and our models confirm that the velocity increases rather steeply near the stellar surface but, at the same time, casts doubts about the uniqueness of its representation.

Most of the optical depths, τ_0, are of the order of or less than unity. This means that, since the wind is optically thin in the Hα line, most of the radiation originates from regions rather close to the stellar photosphere and, therefore, the Hα line is probing the inner layers of the stellar wind. The one exception is P Cyg for which the optical depth is over 200: this fact, combined with the relatively shallow gradient ($\gamma = 0.5$), indicates that the emitting region extends to several stellar radii.

Looking at Table 3, it is apparent that most stars have mass loss rates around 4×10^{-6} $M_\odot$ yr^{-1} to within a factor of 1.5. The accuracy of these determinations is quite good, the uncer-

tainties being lower than 25% in most cases. The most extreme case is P Cyg, whose mass loss rate is about 5 times higher than the average. The $\dot{M}$ values derived in this paper are different from our early estimates presented at the Boulder Workshop on Properties of Hot Luminous Stars (Scuderi et al. 1990) because there the mass loss rates were determined *adopting* guessed values of γ and v_0, whereas here these latter quantities are *determined* from the line profile fitting.

In general, our mass loss rates compare well with other determinations. In particular, for P Cyg, which is a strong source at all wavelengths, our determination is quite close to both the one derived by Abbott, Bieging, & Churchwell (1981) from radio continuum measurements and that of Felli et al. (1985) which is mainly based on near-IR measurements. Also in the case of Cyg OB2 No. 8A (BD +40°4227) the agreement between our determination and those obtained by Leitherer et al. (1982) from similar Hα spectroscopy and by Abbott et al. (1981) from radio continuum measurements is quite remarkable.

Furthermore, our determinations which are based on new observations and ab initio model calculations agree rather well with those obtained by Leitherer (1988) based on a semi-empirical calibration of the $L(\mathrm{H}\alpha)$ versus $\dot{M}$ relationship and on data taken from the literature. On the one hand, this indicates that both the uncertainties introduced by simplifications in our theoretical models are quite modest, say, less than 25%, and that variability, although conspicuous in some cases, is generally contained within levels of $\sim$25% in $\dot{M}$ or, correspondingly, a factor of $\sim$1.6 in the Hα emission. On the other hand, our detailed results justify the success of Leitherer's approach which is based on the assumption that Hα is an optically thin line.

6. CONCLUSIONS

We have started an observational program at the Catania Astrophysical Observatory to study and monitor the Hα emission from early-type stars and determine the properties of their mass loss. Here we have presented the results of a first run of 1988 July in which 12 early-type supergiants in the Cygnus region were observed repeatedly over different nights.

The main results can be summarized as follows.

a. We have found evidence for short-term variability i.e., on a time scale of days, of the mass loss rate of at least three of the 12 program stars. Also, for some of them a comparison with literature data revealed strong long-term (time scale of years) variations.

b. We have also developed simplified models to describe the Hα profile resulting from the combination of photospheric absorption with emission and scattering in the wind. Most of the results can be expressed in an analytical form and allow one to quickly and accurately analyze Hα line observations.

c. By fitting the observed profiles with our models we determine the mass-loss rates and the velocity fields for all stars with accuracies generally better than 25%. Most of the program stars have mass-loss rates around $4 \times 10^{-6}\ M_\odot\ \mathrm{yr}^{-1}$ and velocity fields characterized by a fast initial acceleration up to few hundreds km s^{-1} and a rather gradual increase afterward.

d. We also find that the O3 If star Cyg OB2 No. 7 may be a runaway star, possible companion of a very massive star ($\geq 100\ M_\odot$) which exploded less than 10^5 yr ago.

To conclude, let us stress that Hα observations have proved to be able to provide accurate estimates of the mass loss rate. Considering that Hα observations can easily be made with small telescopes and rather simple instrumentation and require exposure times quite reasonable (in our cases from few seconds to about 20 minutes), it is clear that they provide one of the best tools to make statistical studies of the mass loss from early-type stars.

We wish to thank K. Horne for kindly providing his computer code used to determine the continuum level in our spectra. S. S. acknowledges the warm hospitality of the Space Telescope Science Institute, where part of this work was carried out. This work has been partially supported by the Italian Ministero dell'Università e della Ricerca Scientifica e Tecnologica through grants to the University of Catania and the Catania Astrophysical Observatory.

REFERENCES

Abbott, D. C., Bieging, J. H., & Churchwell, E. 1981, ApJ, 250, 645
Abbott, D. C., Bieging, J. H., Churchwell, E., & Cassinelli, J. P. 1980, ApJ, 238, 196
Auer, L. H., & Mihalas, D. 1972, ApJS, 24, 193
Barlow, M. J., & Cohen, M. 1977, ApJ, 213, 737
Bernat, A. P., & Lambert, D. L. 1978, PASP, 90, 520
Bonanno, G., & Di Benedetto, R. 1990, PASP, 102, 835
Castor, J. I. 1970, MNRAS, 149, 111
Castor, J. I., & Klein, R. I. 1978, ApJ, 220, 902
Castor, J. I., & Lamers, H. J. G. L. M. 1979, ApJS, 39, 481
Conti, P. S. 1974, ApJ, 187, 539
Conti, P. S., & Frost, S. A. 1977, ApJ, 212, 728
Ebbets, D. 1982, ApJS, 48, 399
Felli, M., & Panagia, N. 1981a, A&A, 102, 424
———. 1981b, in Effects of Mass Loss on Stellar Evolution, IAU Symp. 59, ed. C. Chiosi & R. Stalio (Dordrecht: Reidel), 179
Felli, M., Stanga, R., Oliva, E., & Panagia, N. 1985, A&A, 151, 27
Garmany, C. D., Olson, G. L., Conti, P. S., & Van Steenberg, M. E. 1981, ApJ, 250, 660
Groenewegen, M. A. T., & Lamers, H. J. G. L. M. 1989, A&AS, 79, 359
Herbig, G. H. 1975, ApJ, 196, 129
Klein, R. I., & Castor, J. I. 1978, ApJ, 220, 902
Kurucz, R. L. 1979, ApJS, 40, 1
Lamers, H. J. G. L. M., Stalio, R., & Kondo, Y. 1978, ApJ, 223, 207
Leitherer, C. 1988, ApJ, 326, 356
Leitherer, C., Hefele, H., Stahl, O., & Wolf, B. 1982, A&A, 108, 102
Mihalas, D. 1972, NCAR-TN/STR-76.
Panagia, N. 1988, in Galactic and Extragalactic Star Formation, ed. R. E. Pudritz and M. Fich (Dordrecht: Kluwer), 25
Panagia, N., & Felli, M. 1975, A&A, 39, 1
Panagia, N., & Macchetto, F. 1982, A&A, 106, 266
Panagia, N., & Scuderi, S. 1991, in preparation
Peppel, U. 1984, A&AS, 57, 107
Rosendhal, J. D. 1973, ApJ, 186, 909
Scuderi, S., Bonanno, G., Spadaro, D., & Panagia, N. 1990, in Properties of Hot Luminous Stars, ed. C. D. Garmany (San Francisco: ASP), 253
Sobolev, V. V. 1958, in Theoretical Astrophysics, ed. V. A. Ambartsumyan (NY: Pergamon), 482
Striganov, A. R., & Sventitskii, N. S. 1968, in Tables of Spectral Lines of Neutral and Ionized Atoms (New York: Plenum)
Vallée, J. P., & Moffat, A. F. J. 1985, AJ, 90, 315